Generation of mice with conditional ablation of the *Cd40lg* gene.
New insights on the role of CD40L.

Angélica Horrillo[b], Tomás Fontela[a,b], Elena G. Arias-Salgado[a], Dolores Llobat[a], Gracia Porras[a], Matilde S. Ayuso[a,b], and Consuelo González-Manchón[a,b]

[a] Department of Cellular and Molecular Medicine, Centre of Biological Research, CIB-CSIC, Madrid, Spain
[b] CIBER de Enfermedades Raras (CIBERER), Madrid, Spain

Corresponding author: Dr. Consuelo González-Manchón, Department of Cellular and Molecular Medicine, Centro de Investigaciones Biológicas, CIB-CSIC, Calle Ramiro de Maeztu 9, 28040-Madrid, Spain- Tel.: +34918373112-4441; Fax: +34915360432; e-mail: cgmanchon@cib.csic.es

Abstract

CD40 ligand (CD40L) acts as an immune modulator in activated T cells, and mutations in the extracellular domain are associated to X-linked hyper IgM syndrome. A role for platelet CD40L in mediating thrombotic and inflammatory processes in atherosclerosis has also been reported. Using the Cre/loxP recombination technology we generated four knockout lines of mice with deletion of the *Cd40lg* gene restricted to the hematopoietic system. Mouse lines with expression of Cre recombinase driven by the Tie2, Vav1, or CD4 promoters showed *in vivo* ablation of *Cd40lg* in leukocytes and platelets. In contrast, in mice with Cre expression driven by the megakaryocyte lineage-restricted Pf4 promoter, abolition of CD40L expression was observed in megakaryocytes cultured *in vitro*, but not in circulating platelets. Characterization of these animals revealed reduced *in vivo* thrombogenesis and defective activation of washed CD40L-deficient platelets, suggesting that membrane-bound CD40L is involved in the control of haemostasis acting as a platelet co-activator. In addition, we report the practically absence of CD40L in mouse and human endothelial cells, as well as the detection of an exon 3-deleted CD40L transcript in both platelets and leukocytes of mouse and human origin. Finally, compared with their corresponding littermate "floxed" controls, Cre+ mice carrying CD40-deficient leukocytes did not exhibit increased IgM levels, and reduction of IgA and IgG levels was statistically significant only in Tie2-Cre+ mice, suggesting that expression of CD40L in an earlier developmental step may be determinant in the regulation of the class switch recombination process.

Introduction

The ligand of the CD40 receptor, CD40L, is a type II membrane glycoprotein of the tumor necrosis factor ligand (TNFL) superfamily composed of 215 amino acids distributed in three functional domains: a 22 AA intracellular domain, a 24 AA transmembrane domain, and a cysteine-rich extracellular domain containing 215 AA. The sandwich structure of the TNFL homology domain in the extracellular region allows the typical trimeric organization of the members of this family of proteins (Shimadzu et al. 1995). Besides the complete 39 kDa CD40L molecule bound to the plasma membrane, there is a soluble 18 kDa form (sCD40L) that can associate with the complete form of the protein in biologically active heterotrimeric complexes (Graf et al. 1995).

The role of CD40L as an immune modulator is well known. It has been implicated in several immune events including B cell proliferation, differentiation, isotype switching, regulation of stimulatory molecules, activation of antigen presenting cells and modulation of T cell priming (Elgueta et al. 2009). CD40L is also involved in haematopoietic development, including stem and progenitor cells (HSPCs), and it plays a critical role in the differentiation of naïve CD4+ T-cells into different T helper subsets (Seijkens et al. 2010). In humans, mutations in the extracellular domain of CD40L give rise to a rare immunodeficiency disorder, the X-linked hyper-IgM syndrome, characterized by increased susceptibility to infections and defective Ig isotype switching, resulting in low or undetectable serum levels of IgG and IgA, and normal or elevated IgM (Aruffo et al. 1993).

Besides its expression in activated CD4+ T cells, CD40L is also found in a broad range of cells including T cells, B cells, basophils, eosinophils, NK cells, macrophages, dendritic cells, and endothelial cells (Mach et al. 1997; Schonbeck et al. 2000). Moreover, CD40L is constitutively expressed in megakaryocytes, and activated platelets appear to be the primary source of plasma sCD40L (Henn et al. 1998; Inwald et al. 2003). Emerging evidences suggest that platelet CD40L is involved in the adaptive immune response (Elzey et al. 2011) and, also, it may contribute to inflammatory diseases, including atherosclerosis (Nurden 2011; Hassan et al. 2012). Moreover, platelet CD40L has been reported to stabilize arterial thrombi through a mechanism involving interaction with αIIbβ3 integrin (Andre et al. 2002b). Many of these studies were performed using a total CD40L knockout mouse model (Xu et al. 1994), the only CD40L-deficient mice so far reported.

In this work, we intended to study the role of CD40L in different cell types. For this purpose, we have crossed a CD40L "floxed" mouse line (Nowakowski et al. 2011) with four different transgenic mice with restricted expression of Cre recombinase in the hematopoietic system, driven by *Tie2* (the gene for tunica intima endothelial kinase 2), *Vav1* (coding for a guanine nucleotide exchange factor), *CD4* (cluster of differentiation 4), and *Pf4* (coding for the platelet factor 4) promoters. These lines were selected because they express Cre recombinase at different developmental stages, therefore offering additional information on the possibility that CD40L-dependent developmental events could influence the functional response. Evaluation of *in vivo* thrombogenesis and CD40L-deficient platelet activation, as well as determination of serum Ig levels in mice carrying CD40L-deficient leukocytes, provide valuable data on the functional significance of CD40L expression.

Material and Methods

Ethics Statement

All experiments with animals were done in such a way as to minimize animal suffering, according to relevant national and international guidelines ("Guide for Care and Use of Laboratory at the Institute of Laboratory Animal Resources").

The ethics committee of the Center for Biological Research (CSIC) and the grant review board (ANEP) of the Spanish Ministry of Science and Technology specifically approved this study in accordance with the guidelines of the European Community Council Directive 86/609 EEC.

Animals

Mice used in all the experiments were maintained under controlled conditions of light and temperature. $Cd40lg^{f/f}$::Pf4-Cre, $Cd40lg^{f/f}$::Vav-Cre, and $Cd40lg^{f/f}$::CD4-Cre littermates were generated on a mixed C57BL/6-129sv, and $CD40L^{f/f}$::Tie2-Cre on a mixed CD1 genetic background, and were backcrossed for 10 generations with C57BL/6 or CD1 mice, respectively.

To generate mice with a restricted deletion of *Cd40lg* in endothelial and/or hematopoietic cells, mice homozygous for the floxed allele with exons 3-4 flanked by functional loxP sites (Fig. 1A), generated previously (Nowakowski et al. 2011), were crossed to Pf4-Cre mice (generated and kindly gifted by Dr. R.C. Skoda, University Hospital Basel, Switzerland) (Tiedt et al. 2007), Tie2-Cre mice (kindly gifted by Dr. J.L. de la Pompa, National Centre of Biotechnology, Madrid, Spain) (Kisanuki et al. 2001), Vav-Cre mice (generated and kindly gifted by Dr. D. Kioussis, National Institute for Medical Research, London, UK) (de Boer et al. 2003) and CD4-Cre mice (kindly gifted by Dr. M. Raspa (European Mouse Mutant Archive, Roma, Italy) (Lee et al. 2001).

PCR genotyping

Recombination of the *Cd40lg* gene region flanked by the loxP sequences was verified by PCR analysis of genomic DNA. Oligonucleotides loxP-S: 5'-TTTCACTCCAGGTGATGAGG-3' (overlapping intron3-exon4 sequences) and AS-8774: 5'-AATCTAACGTCTCAGCGCCTAT-3' that targets a sequence in intron 4 were used to verify the correct insertion of the right loxP sequence in "floxed" mice. The same antisense primer and S-5669: 5'-ATAAGCACCCACAAAACACACT-3' located in intron 2 were used to confirm the deletion of a DNA fragment comprising exons 3 and 4 in genomic DNA from endothelial cells of Tie2-Cre+ and leukocytes of Vav1- and CD4-Cre+ mice. Deletion of exons 3-4 in genomic DNA from *in vitro* differentiated megakaryocytes was verified with oligonucleotides S-5669 and AS-9514: 5'-GTTAGGTCAATCTCTGGTTATCAC-3' located in intron 4.

For littermate genotyping, tail genomic DNA and oligonucleotides S-6012: 5'-CCAGGGATTCCCAATTGCTAT-3' and AS-6259: 5'-CAAAATTGGTAATAGCAACCTACC-3' were used to verify amplification of a DNA fragment comprising the left loxP sequence, and identification of Cre+ mice was performed by amplification of a DNA fragment with a sense oligonucleotide targeting a sequence of the specific promoter and an antisense primer targeting the *Cre* gene sequence.

RT-PCR analysis of CD40L expression

Total RNA from *in vitro* differentiated mouse megakaryocytes, platelets, peripheral blood mononuclear cells (PBMCs), and $CD4^+$ T cells, and from mouse and human endothelial cells, was obtained using the "High Pure RNA Isolation Kit" from Roche. After removing platelet-rich plasma, peripheral blood was layered onto Histopaque 1083 (Sigma) or LymphoPrep (Progen Biotechnik) for separation of mouse or human PBMCs, respectively. A magnetic bead-based kit from Miltenyi was used to isolate mouse CD4+ T cells from total blood previously treated with hypotonic buffer to lyse red cells.

RT-PCR amplification with oligonucleotides S-ATG: 5'-GCATGATAGAAACATACAG-3' located in exon 1 and AS-TGA: 5'-TGTTCAGAGTTTGAGTAAGCC-3' located in exon 5 confirmed normal sized cDNA in *in vitro* differentiated megakaryocytes from "floxed" mice and the deletion of exons 2-3 in cells from Cre+ mice.

Oligonucleotide pairs with a common antisense primer (AS-TGA) and sense primers S-WT: 5'-TGCAAAAAGGTGATCAGAATC-3' overlapping exons 3 and 4, S-KO: 5'-GAAGACCTTGTCAAGTTCTACA-3' overlapping exons 2 and 5, and S-Sp: 5'-CTTGTCAAGGTGATGAGGA-3' overlapping exons 2 and 4, were designed to amplify similarly sized products corresponding to the normal, exons-2-3-deleted, and exon-3-deleted transcripts, respectively.

RT-PCR analysis was also performed in human platelets, PBMCs, umbilical vein endothelial cells (HUVEC), human microvascular endothelial cell line (HMEC-1), and blood outgrowth endothelial cells established from peripheral blood (BOEC), using the same AS-TGA primer, conserved in the human sequence, and sense primers S-hWT: 5'-TGCAAAAAGGTGATCAGAATC-3' overlapping exons 3 and 4, and S-hSp: 5'-GGCTTTGTGAAGGTGATCA-3' overlapping exons 2 and 4, to amplify similarly-sized products corresponding to the normal and exon-3-deleted transcripts, respectively.

In all RT-PCR assays, amplification of a cDNA fragment of human or mouse β-actin was carried out in parallel to verify that equal amounts of RNA were used ensuring correct normalization of CD40L expression.

All RT-PCR assays were carried out twice, with similar results, using two different mixtures of RNA from at least 3 animal of each genotype.

***In vitro* differentiation of megakaryocytes**

Bone marrow cells were flushed from femurs and tibias with Tyrode's buffer, dissociated and cultured in IMDM with 5% fetal bovine serum, 50 ng/mL TPO, 2 mM L-glutamine, 50 U/mL penicillin, and 50 µg/mL streptomycin. Megakaryocytes were recovered by passing the suspension through a discontinuous density gradient of albumin.

Endothelial cell isolation and culture

Mice lungs from $Cd40lg^{lox/lox}$ and $Cd40lg^{-/-}$ littermates were collected, chopped, digested with 1 mg/ml collagenase A (Roche, 10103578001), filtered through a sterile 18G microlance, and sieved through a cell strainer with 70 µm nylon membrane pore (Beckton and Dickinson). The purification of endothelial cells was carried out by a single negative sorting with anti-CD16/32 antibody (BD Pharmigen, 553142) and a

single positive sorting with anti-ICAM2 antibody (BD Pharmigen, 553326), using Dynabeads sheep anti-rat IgG (Invitrogen, 110.35) and a magnetic particle concentrator (Dynamag^{TM}-15, Invitrogen 123.01D). Endothelial cells were plated on gelatin-coated 60 mm dishes and cultured during 3 days in medium containing DMEM (Gibco, 41966), Hams F-12 (Lonza, BE12-615F), 100 UI/mL penicillin/100 µg/ml streptomycin (Gibco, 15070-063), 20% fetal bovine serum (Sigma F7520), 20 µg/ml endothelial cell growth supplement from bovine neural tissue (ECGS, Sigma E2759) and 0.1 mg/ml of heparin sodium salt (Sigma, H3393). Finally, trypsin-detached cells were labeled with anti-ICAM2-FITC antibody (BD Pharmigen, 557444) and analyzed in a Coulter flow cytometer model EPICS XL. Only cultures with percentages greater that 90% of endothelial cells were used.

Flow cytometry analysis of surface expression of CD40L

Cell suspensions from mouse spleens were prepared by mechanical dissociation. Debris was removed by sedimentation followed by filtration through a 70 µm cell strainer, centrifugation, and resuspension in DMEM-10% FCS. After cell counting, single-cell suspensions from three animals of each genotype were mixed for cell activation assays. Spleen single-cell suspension (10^7 cells) were incubated in the absence or presence of 50 ng/mL PMA and 1 µg/mL ionomycin and, then, washed and stained with anti-CD40L(clon MR1)-PE and anti-CD4(clon GK1.5)-FITC (eBioscience) or isotype-matched antibodies as negative control for 15 minutes at 4ºC, washed, and analyzed in a Coulter flow cytometer model FC500. The experiment was carried out twice with similar results.

Preparation and activation of washed platelets

Citrated blood samples were obtained by cardiac puncture under isofluorane anesthesia. The blood was centrifuged at 100 g for 20 minutes at room temperature. Platelet-rich plasma was removed and centrifuged at 1300 g in the presence of 0.1 µg/mL prostacyclin and 0.02 U/mL apyrase (Sigma) for 5 minutes at room temperature, and washed 3 times with modified Tyrode's buffer containing 0.1 µg/mL prostacyclin and 0.02 U/mL apyrase. The sedimented platelets were finally suspended in Tyrode's buffer containing 0.02 U/mL apyrase and rested for 30 minutes at 37°C prior to stimulation.

The membrane content of surface receptors was determined in washed platelets incubated with FITC-labeled rat anti-mouse integrin αIIbβ3 and GPVI (Emfret Analytics, Eibelstadt, Germany) or control isotype-matched mouse IgGs for 30 minutes at room temperature. The samples were then washed and analyzed by flow cytometry.

To determine the extent of platelets activation, 25 µL of washed platelets (10^6 approximately) suspended in Tyrode's-buffer containing 1 mM $CaCl_2$ were stimulated with 10 µM ADP plus 50 µM epinephrine, or 0.2-1 U/mL thrombin. Activation was assessed by determining P-selectin exposure and αIIbβ3 activation by flow cytometry with 5 µL of FITC-anti-P-selectin (Beckton and Dickinson) or PE-anti-activated αIIbβ3 (JON/A, Emfret Analytics) moAbs.

Thrombogenesis *in vivo*

As previously reported (Pericacho et al. 2011), 100 µL of blood was collected from one of the jugular veins of anesthetized mice into a tube containing 10 µL of 0.129 M sodium citrate. A mixture of

collagen/epinephrine (150 ng collagen type I (Chronolog) and 15 ng epinephrine (SIGMA) per g of mice body weight) was then injected into the same vein and, after 2 minutes, blood was withdrawn from the other jugular vein as indicated above. The number of platelets in both samples was determined using a hemocytometer analyzer Abacus Junior (Diatron Messtechnik GmbH, Austria).

Immunoglobulin measurement by flow cytometry

Immunoglobulin detection in "floxed" and conditional knockout mice from VAV-Cre, Tie2-Cre and CD4-Cre lines was performed with the Mouse Immunoglobulin Isotyping panel 6plex kit (eBioscience, BMS815FF) by flow cytometry, following manufacturer´s instructions. Non-citrated blood was extracted by cardiac puncture of 12-week-old mice. Complete blood was stored overnight at 4ºC and, after centrifugation at maximum speed, serum was collected and used to detect IgA, IgG1, IgG2a, IgG2b, IgG3 and IgM immunoglobulins. Results obtained were analyzed with FlowCytomix Pro Software (eBioscience) to determine immunoglobulin concentration.

Results

CD40L expression in mouse lines with conditional knockout of CD40L in hematopoietic cells

To study the functional consequences of conditional knockout of CD40L, mice bearing two copies of the Cd40lg floxed allele (Fig. 1A) generated as previously described (Nowakowski et al. 2011) were mated with transgenic mouse lines expressing Cre recombinase driven by the promoters of three different genes that are expressed in T cells: *Tie2* (the gene for tunica intima endothelial kinase 2), *Vav1* (coding for a guanine nucleotide exchange factor), and *CD4* (cluster of differentiation 4). The Tie2-Cre line (Kisanuki et al. 2001) produces Cre recombinase in endothelial cells and their progeny, including hematopoietic stem cells (HSC) and blood cells (Hsu et al. 2000); the Vav-iCre line (de Boer et al. 2003) expresses the Cre recombinase specifically in hematopoietic cells but only after HSC formation (He et al. 2008); and the CD4-Cre line allows the Cre-recombinase to act on a later step of T cell development, the CD4+ T cells (Lee et al. 2001), and also in an early step in megakaryocyte maturation (Basch et al. 1996). Using genomic DNA from endothelial cells and leukocytes, we verified the correct insertion of right loxP sequence in "floxed" mice and the deletion of a DNA fragment comprising exons 3 and 4 in Cre+ mice (Fig. 1B-C).

We assessed CD40L expression by RT-PCR analysis of the CD40L transcripts. We then designed oligonucleotide pairs consisting of a common antisense primer located in exon 5 and specific sense primers to amplify the normal or the deleted transcript. As shown in Fig. 2, in the three mouse lines, amplification of the normal transcript using a sense primer overlapping exons 2 and 3 was detected in platelets and leukocytes from control "floxed" mice, but not from Cre+ mice. In contrast, amplification with a sense primer overlapping exons 2 and 5 allowed detection of the deleted transcript only in Cre+ mice. Ablation of the *Cd40lg* gene in all these animals has not apparent effect on phenotype. The rates of growth and fertility were normal and no significant differences were detected in hemogram counts (Table S1).

In order to demonstrate the absence of CD40L protein in targeted cells, spleen cell suspensions from "floxed" and Cre+ mice were stimulated with PMA/ionomycin and the surface expression of CD40L was determined in CD4+ cells by flow cytometry. As shown in Fig. 3, for all three Cre lines, CD40L was clearly detected in "floxed" mice but not in Cre+ mice.

We also generated a fourth mouse line by mating *Cd40lg* $^{f/f}$ mice with mice expressing Cre-recombinase under the control of platelet factor 4 promoter (Pf4) (Tiedt et al. 2007). In contrast to the other mouse lines, the results from semiquantitative RT-PCR analysis in platelets revealed an inefficient Cre-mediated recombination. As shown in Fig. 3A, the deleted transcript was detected in Cre+ mice only after 40 cycles of PCR amplification. Consistent with the scarce amount of the mutant transcript, amounts of amplification products of the normal transcript were similar to those obtained in "floxed" mice. However, efficient Cre-mediated excision of the floxed allele was demonstrated in *in vitro* cultured megakaryocytes. We verified the deletion of a DNA fragment comprising exons 3 and 4 in Cre+ mice (Fig. 1D). Moreover, amplification with oligonucleotides located in exons 1 and 5 yielded a cDNA product corresponding to the normal transcript in megakaryocytes from "floxed" mice and a product corresponding to the transcript with deletion of exons 3-4 in cells from Cre+ mice (Fig. 3B).

Expression of an exon 3-deleted transcript of CD40L in both platelets and leukocytes

During sequence analysis of RT-PCR products we detected an alternative form of CD40L transcript lacking exon 3 in platelets from mice bearing the *Cd40lg* floxed allele. In order to rule out the possibility of aberrant splicing caused by the presence of the 5'-loxP site, introduced 48 bp upstream of exon 3, we designed a sense primer overlapping exons 2 and 4 and analyzed by RT-PCR the relative expression of this alternative transcript. Results in Fig. 5A show that the exon 3-deleted CD40L transcript is present in both platelets and leukocytes from wild type mice of the same genetic backgrounds. In addition, it was also found in platelets and leukocytes of human origin (Fig. 5B). When compared with expression of the full-length transcript, we estimated that it represents a minor proportion (less than 5%) of total CD40L transcripts (Fig. 5). Skipping of exon 3 results in frameshift and premature stop codon 36 bp downstream. Thus, the aberrant transcript is predicted to encode a protein carrying an abnormal and severily truncated amino acid composition at the extracellular aminoterminal region.

CD40L expression in mouse and human endothelial cells

Early reports on CD40L expression have led to the general consent that CD40L is expressed in endothelial cells, at least of human origin (Mach et al. 1997; Schonbeck et al. 2000). In the present study, RT-PCR of total RNA from mouse lung vascular endothelial cells (MLEC) revealed that CD40L expression is not detectable after 45 cycles of amplification (Fig. 6A). We also failed to detect CD40L in total RNA from human umbilical vascular endothelial cells (HUVEC) and human blood outgrowth endothelial cells **(**BOEC**)** (Fig. 6B). It was only detectable, although scarcely when compared with its expression in leukocytes and platelets, in RNA from human dermal microvascular endothelial cells **(**HMEC-1**)** (Fig. 6B).

***In vivo* thrombogenesis and *in vitro* platelet activation in CD40L knockout mice**

Studies carried out with the *Cd40lg*$^{-/-}$ mouse model (Xu et al. 1994) show a normal hemostasis. However, alteration in thrombus formation (Andre et al. 2002a) has been reported indicating a role of CD40L in protection against thrombosis. Platelets seem to be the main source of sCD40L and a decrease in the concentration of sCD40L inside the thrombus has been related with the thrombogenic defect of the *Cd40lg*$^{-/-}$ mice (Prasad et al. 2003). We performed *in vivo* thrombogenesis experiments by inducing pulmonary thromboembolism by intravenous administration of collagen plus epinephrine. Results summarized in Fig. 7 indicate that Vav-iCre+ mice display a significantly smaller decrease in circulating platelets two minutes after the administration of agonists than Vav-iCre- animals, indicating that CD40L-deficient mice have a decreased thromboembolic response. However, no significant differences were observed in Tie2-Cre+ and CD4-Cre+ mice.

A role for CD40L in fibrin clot formation can be excluded in view that Cre+ mice of the three lines showed similar values of prothrombin time (PT) and activated partial thromboplastin time (aPTT) than their littermate "floxed" controls (Table S2).

Washed CD40L-deficient platelets obtained from the three mouse lines under study show a significant decrease of αIIbβ3 activation in response to thrombin, as determined by the binding of JON/A antibody

that selectively binds to the high affinity conformation of mouse αIIbβ3 (Fig. 8A). Although platelet activation in response to ADP/epinephrine was also reduced in all Cre+ mice, the effect was statistically significant only in platelets from Vav-Cre+ mice. These mice also showed reduced P-selectin release after thrombin stimulation (Fig. 8B). These effects were not due to decreased surface expression of αIIbβ3 and GPVI receptors (Table S3).

Serum immunoglobulin levels in CD40L deficient mice

One of the characteristic features of X-linked hyper IgM syndrome is the alteration in the serum immunoglobulin phenotype (Aruffo et al. 1993). Serum from patients contains elevated levels of IgM, and low to undetectable levels of other immunoglobulin isotypes, including IgG. To determine whether CD40L deficiency associates in mice with a similar phenotype, we determined the immunoglobulin levels in serum from eight control "floxed" and eight Cre+ mice of each Cre line. Table 1 shows that the alterations in the serum levels of Igs varied in the different mouse lines. Tie-Cre+ mice have levels of IgA, IgG1, IgG2a, IgG3 and IgM significantly lower than their littermate "floxed" controls. However, in the Vav-iCre line only IgM levels are significantly reduced while a subset of IgG (IgG1) is significantly increased. Furthermore, in the CD4-Cre line, CD40L knockout does not induce remarkable variations of any of the Igs tested.

Discussion

At present, the only available mouse line deficient for CD40L is a total knockout model generated by replacing a 506-bp DNA fragment containing part of exon 4 with the pCM1 gene in an opposite direction (Xu et al. 1994). These mice have been used to explore the role of CD40-CD40L interaction on different aspects of the immune response as well as on atherogenic and inflammatory processes (Wolf et al. 2012; Lievens et al. 2010).

We have recently generated a Cd40lg "floxed" mouse line in which Cd40lg alleles carry loxP sites flanking a DNA fragment comprising exons 3-4 (Nowakowski et al. 2011). In the present study, we have crossed these animals with three different Cre mouse lines (Tie2-Cre, Vav-iCre, and CD4-Cre) in order to explore the effect of restricting expression of CD40L at different steps of hematopoietic development. Efficiency of Cre-mediated ablation of Cd40lg in lymphocytes and platelets was assessed by RT-PCR analysis of CD40L transcripts. The normal transcript was not found in Cre+ mice, indicating efficient Cre-mediated recombination. Although we have not performed a precise quantitative determination of the CD40L-mRNA levels, the semiquantitative RT-PCR analysis indicates that the amounts of normal and deleted transcripts detected in cells from "floxed" and Cre+ mice, respectively, were similar. The mutant transcript is predicted to produce a protein carrying an abnormal and severely truncated extracellular region lacking the CD40 receptor-binding domain. A similarly truncated CD40L protein has been described previously in a patient causing X-linked hyper IgM syndrome through a dominant negative inhibition of CD40L trimeric complex formation (Zhu et al. 2001). Although, given the relatively high expression of the deleted transcript in our Cre+ mice, we cannot exclude that these animals express significant amounts of a dysfunctional CD40L protein, the flow cytometry analysis of CD4+ T cells stimulated with PMA/ionomycin indicates that CD40L is practically absent in cells from Cre+ mice.

The role of platelet CD40L in thrombosis (Inwald et al. 2003; Prasad et al. 2003) and, also, its emerging function in both innate and adaptive immunity (Semple et al. 2011; Li et al. 2012), inflammation (Nurden 2011; Wolf et al. 2012), and atherosclerosis (Elzey et al. 2011; Wolf et al. 2012; Lievens et al. 2010; Semple et al. 2011; Li et al. 2012) prompted us to develop a mouse line with megakaryocytic specific ablation of CD40L, by using Pf4-Cre mice. Although the floxed Cd40lg allele was efficiently excised in *in vitro* differentiated megakaryocytes from Pf4-Cre+ mice, we found that circulating platelets from control "floxed" and Cre+ mice carry similar amounts of the CD40L normal transcript, suggesting a practically total failure of Cre to induce recombination *in vivo*. Other genes expressed in megakaryocyte/platelet, like β1 integrin or podocalyxin, have been successfully excised using the same Pf4-Cre transgenic mouse line (Tiedt et al. 2007; Pericacho et al. 2011), which discards a deficient expression of Cre recombinase. Persistence of a Cre-recombination episomal product has been reported to be the cause of absolute lack of protein loss in an inducible Cre mouse model where efficient DNA deletion occurred (Turlo et al. 2010). This possibility is unlikely in our case; although we have not confirmed that loxP alleles were not appropriately targeted during *in vivo* differentiation of megakaryocytes, the almost undetectable levels of deleted transcripts in platelets (Fig. 4A), compared with those obtained in the other Cre mouse lines (Fig. 2A-C), points to a deficient Cre-mediated excision. Thus, these results indicate that, for unexplained reasons, Pf4-driven Cre expression fails to excise this Cd40lg floxed allele during *in vivo* differentiation of megakaryocytes, and highlight the need of validate

protein depletion *in vivo* for every novel Cre/loxP combination.

The decreased pulmonary thrombogenic response observed *in vivo* in Vav-iCre+ mice supports the role of CD40L in thrombus formation and/or stability. This role has been claimed to be mediated by sCD40L in humans. Several pathologies involving thrombotic risk (hypercholesterolaemia, diabetes, stroke or acute coronary syndromes) show platelet activation and high levels of sCD40L (Tousoulis et al, 2010; Nurden, 2011). We show that activation of αIIbβ3 in response to thrombin was significantly reduced in washed platelets from the three Cre mouse lines. This effect was more pronounced in Vav-iCre+ mice, which also showed deficient integrin activation upon ADP/epinephrine stimulation, reduced P-selectin exposure in response to thrombin, and a diminished thrombogenic response *in vivo*. These effects were not due to defective expression of αIIbβ3. Previous studies addressing the function of platelet CD40L have shown that the absence of CD40L impairs thrombus stability and delays arterial occlusion *in vivo* (Andre et al. 2002b; Prasad et al. 2003). However, isolated platelets stimulated with soluble CD40L (sCD40L) have yielded somewhat differing conclusions on CD40L-mediated platelet activation. Addition of sCD40L to platelets has been shown to promote CD40-mediated exposure of P-selectin and granule release, but not platelet aggregation (Inwald et al. 2003). By contrast, activation of αIIbβ3 and platelet aggregation under high shear, mediated by the binding of sCD40L to αIIbβ3, has been reported after addition of sCD40L to CD40-deficient platelets (Andre et al. 2002b; Prasad et al. 2003). Our experiments showing defective activation of washed CD40L-deficient platelets add further insights into the functional significance of platelet CD40L and suggest that membrane-bound CD40L is involved in the control of hemostasis acting as a platelet co-activator.

In humans, mutations in the *Cd40lg* gene cause X-linked hyper IgM (X-HIGM) immunodeficiency syndrome, characterized by recurrent infections, low levels of serum IgG, IgA and IgE, and elevated or normal levels of serum IgM due to defective immunoglobulin isotype switching (Levy et al. 1997). Consistent with a previous study carried out in a total knockout mouse model (Xu et al. 1994), conditional knockout of the *Cd40lg* gene did not associate to increased levels of serum IgM in any of the three mouse lines expressing Cre in hematopoietic cells. By contrast, IgM levels were significantly reduced in Tie2-Cre+ and Vav-iCre+ mice. In consonance with these data, a recent report has revealed that about 50% of X-HIGM patients do not present increased IgM and in approximately 6.4% of the cases the IgM levels are decreased, suggesting that patients with total hypogammaglobulinemia may not have undergone diagnostic procedures for X-HIGM and detection of Cd40lg mutations (Heinold et al. 2010). Determination of serum levels of IgA and IgG subclasses also yielded unexpected results. Vav-iCre+ and CD4-Cre+ mice showed no significant changes, and the decrease detected in Tie2-Cre+ mice, although significant, may not be sufficient to have functional relevance. It is known that CD40L is involved in haematopoietic development, including stem and progenitor cells (HSPCs), T-cell, B-cell, and dendritic cell progenitors, and it plays a critical role in the differentiation of naïve CD4+ T-cells into different T helper subsets (Seijkens et al. 2010). Expression of CD40L in one of these subpopulations, the T follicular helper cells, is thought to be essential to mediate antibody class switching through the interaction with its receptor, CD40, in mature B cells (Aversa et al. 1994). Our study shows that abolishing expression of CD40L at different steps of hematopoietic cell development does not seem to have a significant impact on class switch recombination suggesting that, at least in mouse, expression of

CD40L in an earlier stage of development may be determinant in the regulation of this process. The significant decrease of IgA and IgG in mice expressing Cre under the Tie2 promoter, activated earlier than Vav1 and CD4 promoters during development, supports this possibility. Alternatively, as observed in an increasing number of mouse models (Montagutelli 2000; Jelcick et al. 2011), it may reflect the difference between C57BL/6-129sv and CD1 genetic backgrounds. Finally, even in case the deleted CD40L transcript expressed in Cre+ mice was translated into a protein, the absence of CD40 binding-domain would preclude its functionality to induce class switch recombination.

Finally, it is worthy to mention that, in contrast to previous reports (Mach et al. 1997; Wagner et al. 2004), we have failed to detect CD40L expression in mouse and human endothelial cells. Scarce RNA expression was only found in a human microvascular endothelial cell line (HMEC-1). Although CD40L expression could be upregulated in inflammatory contexts (Reul et al. 1997; Geraldes et al. 2006), our results suggest that endothelial CD40L has not functional relevance in basal conditions.

In summary, we have established three novel mouse lines with conditional knockout of the Cd40lg gene in the hematopoietic system and verified the efficient Cre-mediated deletion of CD40L in targeted cells. In contrast, ablation of Cd40lg was only observed in *in vitro* differentiated megakaryocytes in a fourth mouse model with Cre expression restricted to the megakaryocyte lineage. Mice carrying CD40L-deficient leukocytes do not exhibit increased levels of serum IgM, and reduction of IgA and IgG levels was statistically significant only in Tie2-Cre+ mice. Our results also show defective activation of washed CD40L-deficient platelets and reduced *in vivo* thrombogenesis, adding further insights into the functional significance of platelet CD40L. Finally, we report the practically absence of CD40L in mouse and human endothelial cells and, also, the detection of an exon 3-deleted CD40L transcript in both platelets and leukocytes of mouse and human origin.

Acknowledgements

CIBER de Enfermedades Raras (CIBERER) is an initiative of the Spanish Health Institute Carlos III (ISCIII).

The work was funded with grants SAF2007-61701 and BFU2010-15237 from the Spanish Plan of Research & Development, and grant PIE 201020E018 from CSIC.

References

Andre P, Nannizzi-Alaimo L, Prasad SK, Phillips DR (2002a) Platelet-derived CD40L: the switch-hitting player of cardiovascular disease. Circulation 106 (8):896-899

Andre P, Prasad KS, Denis CV, He M, Papalia JM, Hynes RO, Phillips DR, Wagner DD (2002b) CD40L stabilizes arterial thrombi by a beta3 integrin-dependent mechanism. Nature Med 8 (3):247-252

Aruffo A, Farrington M, Hollenbaugh D, Li X, Milatovich A, Nonoyama S, Bajorath J, Grosmaire LS, Stenkamp R, Neubauer M, et al. (1993) The CD40 ligand, gp39, is defective in activated T cells from patients with X-linked hyper-IgM syndrome. Cell 72 (2):291-300

Aversa G, Punnonen J, Carballido JM, Cocks BG, de Vries JE (1994) CD40 ligand-CD40 interaction in Ig isotype switching in mature and immature human B cells. Sem Immunol 6 (5):295-301

Basch RS, Dolzhanskiy A, Zhang XM, Karpatkin S (1996) The development of human megakaryocytes. II. CD4 expression occurs during haemopoietic differentiation and is an early step in megakaryocyte maturation. Br J Haematol 94 (3):433-442

de Boer J, Williams A, Skavdis G, Harker N, Coles M, Tolaini M, Norton T, Williams K, Roderick K, Potocnik AJ, Kioussis D (2003) Transgenic mice with hematopoietic and lymphoid specific expression of Cre. Eur J Immunol 33 (2):314-325

Elgueta R, Benson MJ, de Vries VC, Wasiuk A, Guo Y, Noelle RJ (2009) Molecular mechanism and function of CD40/CD40L engagement in the immune system. Immunol Rev 229 (1):152-172

Elzey BD, Ratliff TL, Sowa JM, Crist SA (2011) Platelet CD40L at the interface of adaptive immunity. Thromb Res 127 (3):180-183

Geraldes P, Gagnon S, Hadjadj S, Merhi Y, Sirois MG, Cloutier I, Tanguay JF (2006) Estradiol blocks the induction of CD40 and CD40L expression on endothelial cells and prevents neutrophil adhesion: an ERalpha-mediated pathway. Cardiovasc Res 71 (3):566-573

Graf D, Muller S, Korthauer U, van Kooten C, Weise C, Kroczek RA (1995) A soluble form of TRAP (CD40 ligand) is rapidly released after T cell activation. Eur J Immunol 25 (6):1749-1754

Hassan GS, Merhi Y, Mourad M (2012) CD40 Ligand: A neo-inflammatory molecule in vascular diseases. Immunobiology 217:521-532

He C, Hu H, Braren R, Fong SY, Trumpp A, Carlson TR, Wang RA (2008) c-myc in the hematopoietic lineage is crucial for its angiogenic function in the mouse embryo. Development 135 (14):2467-2477

Heinold A, Hanebeck B, Daniel V, Heyder J, Tran TH, Dohler B, Greil J, Muller FM (2010) Pitfalls of "hyper"-IgM syndrome: a new CD40 ligand mutation in the presence of low IgM levels. A case report and a critical review of the literature. Infection 38 (6):491-496

Henn V, Slupsky JR, Grafe M, Anagnostopoulos I, Forster R, Muller-Berghaus G, Kroczek RA (1998) CD40 ligand on activated platelets triggers an inflammatory reaction of endothelial cells. Nature 391 (6667):591-594

Hsu HC, Ema H, Osawa M, Nakamura Y, Suda T, Nakauchi H (2000) Hematopoietic stem cells express Tie-2 receptor in the murine fetal liver. Blood 96 (12):3757-3762

Inwald DP, McDowall A, Peters MJ, Callard RE, Klein NJ (2003) CD40 is constitutively expressed on platelets and provides a novel mechanism for platelet activation. Circ Res 92 (9):1041-1048

Jelcick AS, Yuan Y, Leehy BD, Cox LC, Silveira AC, Qiu F, Schenk S, Sachs AJ, Morrison MA, Nystuen AM, DeAngelis MM, Haider NB (2011) Genetic variations strongly influence phenotypic outcome in the mouse retina. PloS one 6 (7):e21858

Kisanuki YY, Hammer RE, Miyazaki J, Williams SC, Richardson JA, Yanagisawa M (2001) Tie2-Cre transgenic mice: a new model for endothelial cell-lineage analysis in vivo. Dev Biol 230 (2):230-242

Lee PP, Fitzpatrick DR, Beard C, Jessup HK, Lehar S, Makar KW, Perez-Melgosa M, Sweetser MT, Schlissel MS, Nguyen S, Cherry SR, Tsai JH, Tucker SM, Weaver WM, Kelso A, Jaenisch R, Wilson CB (2001) A critical role for Dnmt1 and DNA methylation in T cell development, function, and survival. Immunity 15 (5):763-774

Levy J, Espanol-Boren T, Thomas C, Fischer A, Tovo P, Bordigoni P, Resnick I, Fasth A, Baer M, Gomez L, Sanders EA, Tabone MD, Plantaz D, Etzioni A, Monafo V, Abinun M, Hammarstrom L, Abrahamsen T, Jones A, Finn A, Klemola T, DeVries E, Sanal O, Peitsch MC, Notarangelo LD (1997) Clinical spectrum of X-linked hyper-IgM syndrome. J Pediatr-US 131 (1 Pt 1):47-54

Li C, Li J, Li Y, Lang S, Yougbare I, Zhu G, Chen P, Ni H (2012) Crosstalk between platelets and the Immune system: Old systems with new discoveries. Adv Hematol 2012:384685

Lievens D, Zernecke A, Seijkens T, Soehnlein O, Beckers L, Munnix IC, Wijnands E, Goossens P, van Kruchten R, Thevissen L, Boon L, Flavell RA, Noelle RJ, Gerdes N, Biessen EA, Daemen MJ, Heemskerk JW, Weber C, Lutgens E (2010) Platelet CD40L mediates thrombotic and inflammatory processes in atherosclerosis. Blood 116 (20):4317-4327

Mach F, Schonbeck U, Sukhova GK, Bourcier T, Bonnefoy JY, Pober JS, Libby P (1997) Functional CD40 ligand is expressed on human vascular endothelial cells, smooth muscle cells, and macrophages: implications for CD40-CD40 ligand signaling in atherosclerosis. Proc Natl Acad Sci US 94 (5):1931-1936

Montagutelli X (2000) Effect of the genetic background on the phenotype of mouse mutations. J Am Soc Nephrol 11 Suppl 16:S101-105

Nowakowski A, Alonso-Martin S, Arias-Salgado EG, Fernandez D, Vilar M, Ayuso MS, Parrilla R (2011) Megakaryocyte gene targeting mediated by restricted expression of recombinase Cre. Thromb Haemost 105 (1):138-144

Nurden AT (2011) Platelets, inflammation and tissue regeneration. Thromb Haemost 105 Suppl 1:S13-33

Pericacho M, Alonso-Martin S, Larrucea S, Gonzalez-Manchon C, Fernandez D, Sanchez I, Ayuso MS, Parrilla R (2011) Diminished thrombogenic responses by deletion of the Podocalyxin gene in mouse megakaryocytes. PloS one 6 (10):e26025

Prasad KS, Andre P, He M, Bao M, Manganello J, Phillips DR (2003) Soluble CD40 ligand induces beta3 integrin tyrosine phosphorylation and triggers platelet activation by outside-in signaling. Proc Natl Acad Sci US 100 (21):12367-12371

Reul RM, Fang JC, Denton MD, Geehan C, Long C, Mitchell RN, Ganz P, Briscoe DM (1997) CD40 and CD40 ligand (CD154) are coexpressed on microvessels in vivo in human cardiac allograft rejection. Transplantation 64 (12):1765-1774

Schonbeck U, Mach F, Libby P (2000) CD154 (CD40 ligand). Int J Biochem Cell Biol 32 (7):687-693

Seijkens T, Engel D, Tjwa M, Lutgens E (2010) The role of CD154 in haematopoietic development. Thromb Haemost 104 (4):693-701

Semple JW, Italiano JE, Jr., Freedman J (2011) Platelets and the immune continuum. Nat Rev Immunol 11 (4):264-274

Shimadzu M, Nunoi H, Terasaki H, Ninomiya R, Iwata M, Kanegasaka S, Matsuda I (1995) Structural organization of the gene for CD40 ligand: molecular analysis for diagnosis of X-linked hyper-IgM syndrome. Biochim Biophys Acta 1260 (1):67-72

Tiedt R, Schomber T, Hao-Shen H, Skoda RC (2007) Pf4-Cre transgenic mice allow the generation of lineage-restricted gene knockouts for studying megakaryocyte and platelet function in vivo. Blood 109 (4):1503-1506

Tousoulis D, Androulakis E, Papageorgiou N, Briasoulis A, Siasos G, Antoniades C, Stefanadis, C (2010) From atherosclerosis to acute coronary syndromes: the role of soluble CD40 ligand. Trends Cardiovasc Med 20:153–164

Turlo KA, Gallaher SD, Vora R, Laski FA, Iruela-Arispe ML (2010) When Cre-mediated recombination in mice does not result in protein loss. Genetics 186 (3):959-967

Wagner AH, Guldenzoph B, Lienenluke B, Hecker M (2004) CD154/CD40-mediated expression of CD154 in endothelial cells: consequences for endothelial cell-monocyte interaction. Arterioscl Thromb Vasc Biol 24 (4):715-720

Wolf D, Jehle F, Ortiz Rodriguez A, Dufner B, Hoppe N, Colberg C, Lozhkin A, Bassler N, Rupprecht B, Wiedemann A, Hilgendorf I, Stachon P, Willecke F, Febbraio M, von zur Muhlen C, Binder CJ, Bode C, Zirlik A, Peter K (2012) CD40L deficiency attenuates diet-induced adipose tissue inflammation by impairing immune cell accumulation and production of pathogenic IgG-antibodies. PloS one 7 (3):e33026

Xu J, Foy TM, Laman JD, Elliott EA, Dunn JJ, Waldschmidt TJ, Elsemore J, Noelle RJ, Flavell RA (1994) Mice deficient for the CD40 ligand. Immunity 1 (5):423-431

Zhu X, Chung I, O'Gorman MR, Scholl PR (2001) Coexpression of normal and mutated CD40 ligand with deletion of a putative RNA lariat branchpoint sequence in X-linked hyper-IgM syndrome. Clin Immunol 99 (3):334-339

Legends to the figures

Figure 1. Gene targeting and conditional deletion of exons 3-4 of the Cd40lg **gene.** A) Restriction map of the targeting vector, floxed allele, and null allele. Open boxes represent exons numbered as indicated. Neomycin (neo) and thymidine kinase (tk) are positive and negative selection cassettes, respectively. Restriction sites: B, NotI; S, SpeI; X, XhoI; Ss, Sse8387I; A, AscI; E, EcoRI. The arrows indicate the location of oligonucleotides used for PCR genotyping. B) Oligonucleotides loxP-S (1) and AS-8774 (2) amplify a 589 bp DNA fragment in MLECs from "floxed" mice (lane 2) and in total leukocytes from CD4-Cre+ and "floxed" mice (lanes 5 and 6), but not in MLECs from Tie2-Cre+ (lane 1), in total leukocytes from Vav1-Cre+ (lane 3), and in CD4+ leukocytes from CD4-Cre+ (lane 4) mice. C) Oligonucleotides S-5669 (3) and AS-8774 (2) amplify a 868 bp product in MLECs from Tie2-Cre+ mice (lane 1) and in total leukocytes from Vav1-Cre+ and CD4-Cre+ mice (lanes 3 and 4), but not in MLECs from "floxed" mice (lane 2) and in leukocytes from "floxed" mice (lane 5). D) Oligonucleotides S-5669 (3) and AS-9514 (4) amplify a 1608 bp product in *in vitro* differentiated megakaryocytes from PF4-Cre+ mice (lanes 1 and 2) but not from "floxed" mice (lanes 3 and 4).

Figure 2. RT-PCR analysis of CD40L expression in platelets and leukocytes of mice expressing Cre recombinase under the control of Tie2, Vav1, or CD4 promoter. Total RNA from platelets (A, B, and C) PBMCs (D and E) and CD4+ T cells (F) of "floxed" (lanes 1) and Cre+ mice (lanes 2) was used for RT-PCR amplification of the wild type and deleted transcripts of CD40L, using a common antisense primer and specific sense primers, as described in "Methods". The experiments were perfomed twice with similar results.

Figure 3. Flow cytometry analysis of surface expression of CD40L in splenic $CD4^+$ T cells. Spleen single-cell suspension (10^7 cells) were incubated without or with 50 ng/mL PMA plus 1 μg/mL ionomycin and, then, stained with anti-CD4-FITC and anti-CD40L-PE or isotype-matched antibodies as negative control, and analyzed by flow cytometry as described in "Methods". Histograms from a cell mixture of three mice in each group are shown. For clarity, histograms of untreated cells have been omitted. The experiment was carried out twice with similar results.

Figure 4. RT-PCR analysis of CD40L expression in platelets and *in vitro* differentiated megakaryocytes of mice expressing Cre under the control of Pf4 promoter. A) Total RNA from platelets of wild type (lanes 1), "floxed" (lanes 2) and Cre+ mice (lanes 3) was used for RT-PCR amplification of the wild type and deleted transcripts of CD40L, using a common antisense primer and specific sense primers, as described in "Methods". B) Total RNA from bone marrow cells differentiated to megakaryocytes was used for RT-PCR amplification of CD40L using sense and antisense primers located in exons 1 and 5, respectively, as described under "Methods". The experiments were perfomed twice with similar results.

Figure 5. Detection of an exon 3-deleted transcript in platelets and leukocytes of mouse and human origin. Total RNA from platelets and PBMCs of mouse (A) and human (B) was used for RT-PCR amplification of cDNA fragments of CD40L corresponding to the full-length and exon 3-deleted transcripts, using a common antisense primer and specific sense primers as described under "Methods". The experiments were perfomed twice with similar results.

Figure 6. RT-PCR analysis of CD40L expression in endothelial cells of mouse and human origin. Total RNA from mouse leukocytes and lung endothelial cells (MLEC) (A) and from human leukocytes and endothelial cell lines (B) was used for RT-PCR analysis of CD40L expression as described under "Methods". Abbreviations used: HUVEC, human umbilical endothelial cells; HMEC-1, human microvascular endothelial cells; BOEC, blood outgrowth endothelial cells. The experiments were perfomed twice with similar results.

Figure 7. Relative fall in circulating platelets induced by the i.v. administration of collagen/epinephrine. Blood was collected from the jugular vein followed by i.v. injection of a mixture of collagen and epinephrine and, after two minutes, blood was withdrawn from the contralateral vein and the platelet count in both samples determined using a hemocytometer as described in "Methods". The data represent the percent of reduction in the number of circulating platelets and are mean values +/- SEM of at least 6 animals. The Anderson-Darling test was used to verify normal distribution of data. The significance of the results was assessed by two tailed, unpaired, t-test. ns, non significant.

Figure 8. Platelet activation of CD40L-deficient platelets. Washed platelets were estimulated with 10 μM ADP/ 50 μM epinephrin (Epi) or 0.2-1 U/mL thrombin (TB), and the binding of specific antibodies againts activated αIIbβ3 (A) or P-selectin (B) was determined by flow cytometry. The results are mean values +/- SEM of at least 6 animals. The Anderson-Darling test was used to verify normal distribution of data. By two tailed, unpaired, t-test: * $P<0.05$; ** $P<0.005$; ns, non significant.

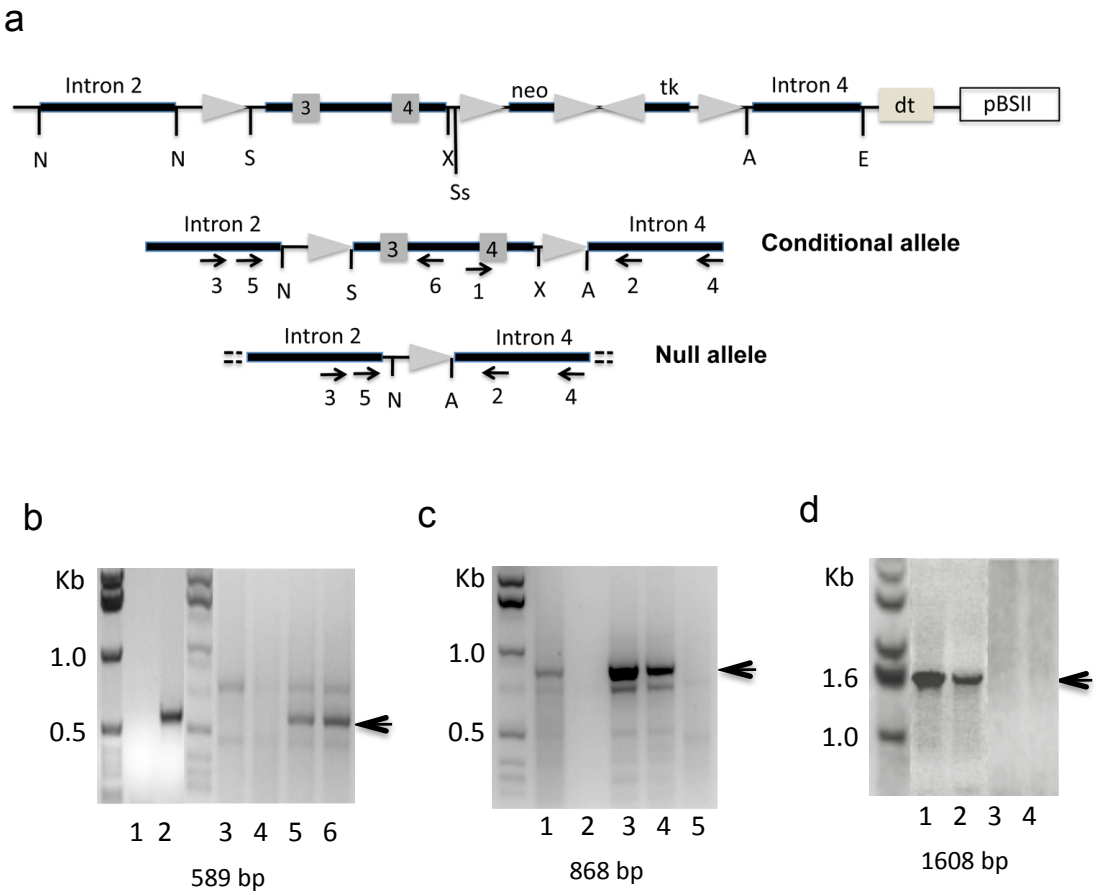
a
Intron 2
3
4
neo
tk
Intron 4
dt
pBSII
N
N
S
X
Ss
A
E
Intron 2
Intron 4
Conditional allele
3
5
N
S
6
1
X
A
2
4
Intron 2
Intron 4
Null allele
3
5
N
A
2
4
b
Kb
1.0
0.5
1 2 3 4 5 6
589 bp
c
Kb
1.0
0.5
1 2 3 4 5
868 bp
d
Kb
1.6
1.0
1 2 3 4
1608 bp

Fig. 1

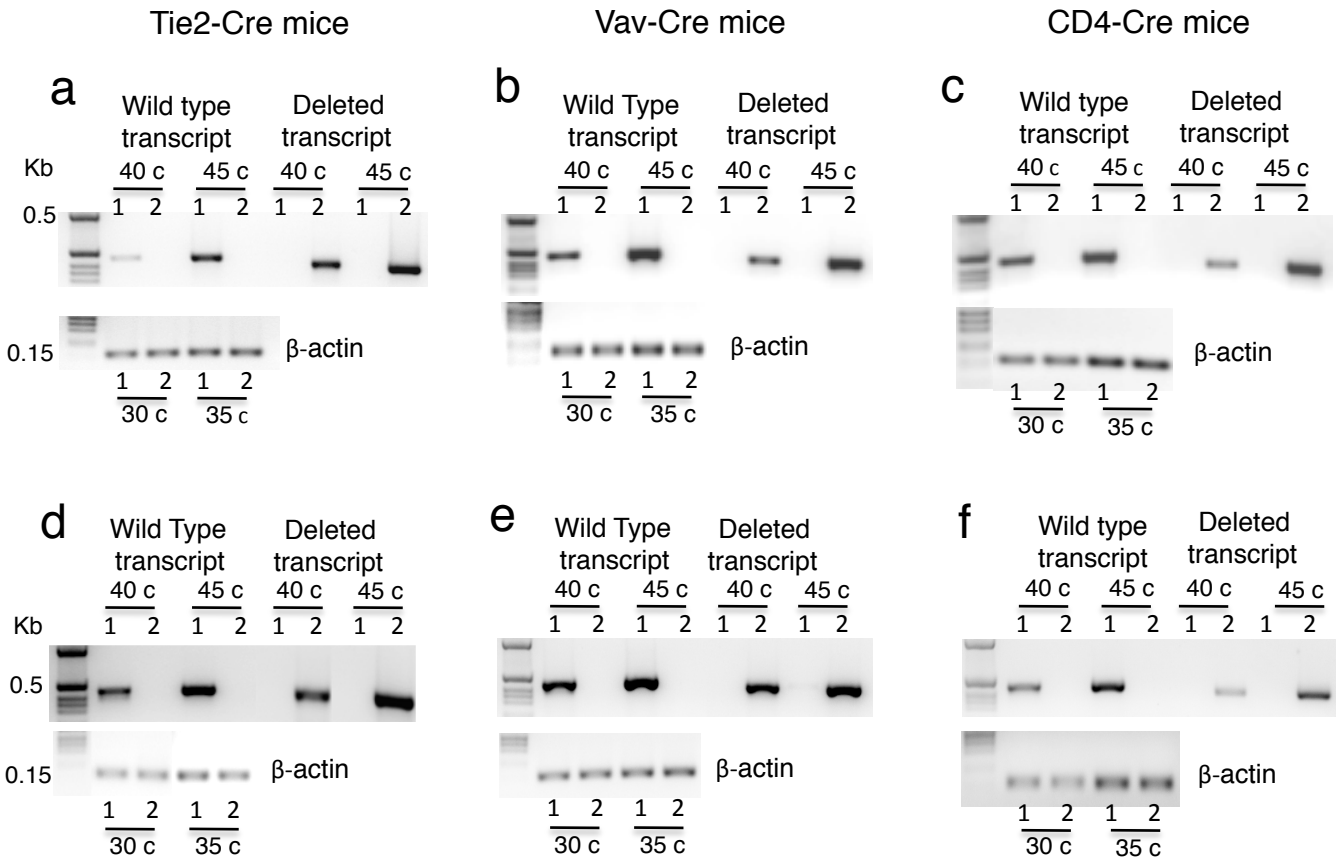
Tie2-Cre mice
Vav-Cre mice
CD4-Cre mice
a
b
c
d
e
f
Wild type transcript
Deleted transcript
Wild Type transcript
Kb
0.5
0.15
40 c
45 c
1 2
β-actin
30 c
35 c

Fig. 2

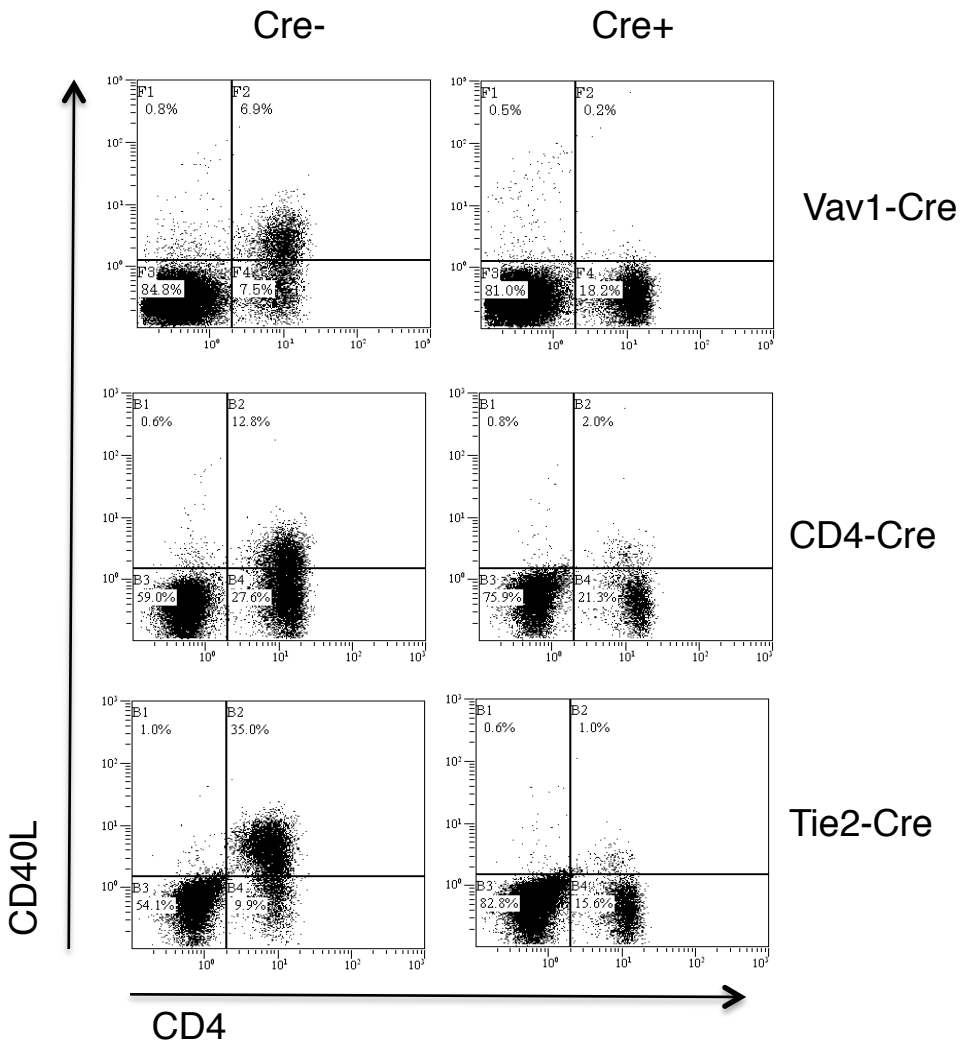
Cre-
Cre+
Vav1-Cre
CD4-Cre
Tie2-Cre
CD40L
CD4
F1 0.8%
F2 6.9%
F3 84.8%
F4 7.5%
F1 0.5%
F2 0.2%
F3 81.0%
F4 18.2%
B1 0.6%
B2 12.8%
B3 59.0%
B4 27.6%
B1 0.8%
B2 2.0%
B3 75.9%
B4 21.3%
B1 1.0%
B2 35.0%
B3 54.1%
B4 9.9%
B1 0.6%
B2 1.0%
B3 82.8%
B4 15.6%

Fig. 3

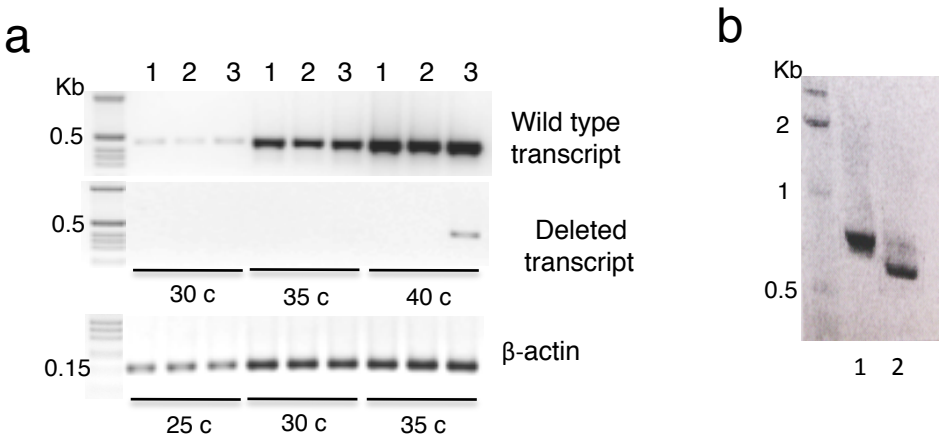
a
1 2 3 1 2 3 1 2 3
Kb
0.5
Wild type
transcript
0.5
Deleted
transcript
30 c
35 c
40 c
0.15
β-actin
25 c
30 c
35 c
b
Kb
2
1
0.5
1 2

Fig. 4

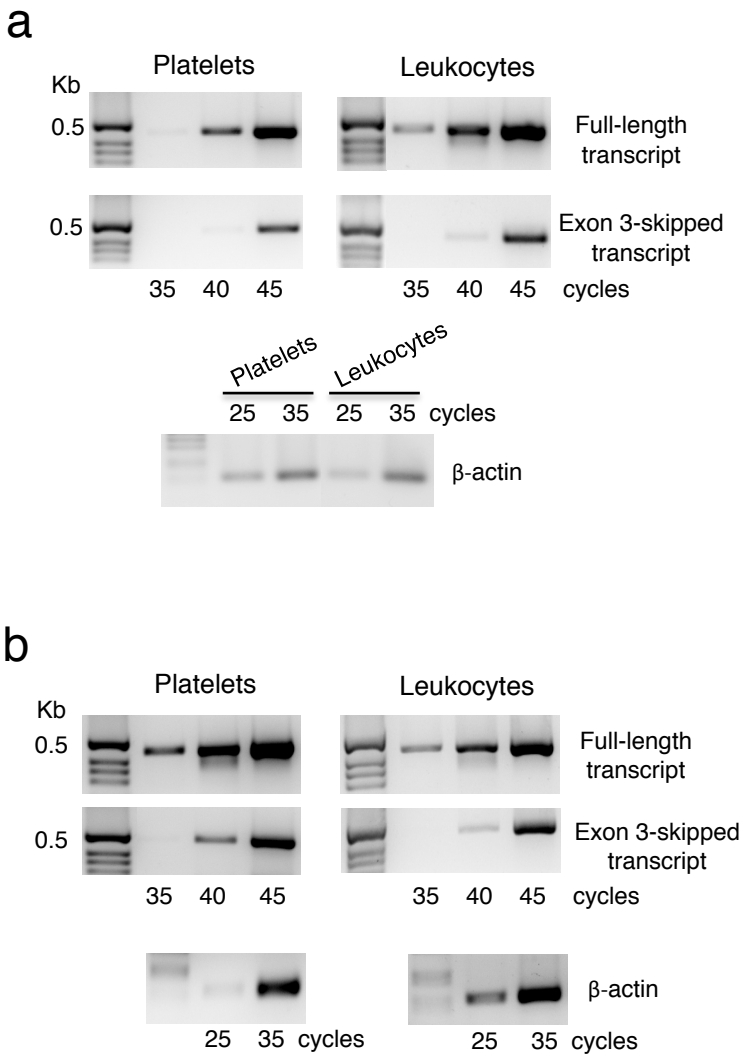
a
Platelets
Leukocytes
Kb
0.5
Full-length transcript
0.5
Exon 3-skipped transcript
35 40 45
35 40 45 cycles
Platelets
Leukocytes
25 35 25 35 cycles
β-actin
b
Platelets
Leukocytes
Kb
0.5
Full-length transcript
0.5
Exon 3-skipped transcript
35 40 45
35 40 45 cycles
β-actin
25 35 cycles
25 35 cycles

Fig. 5

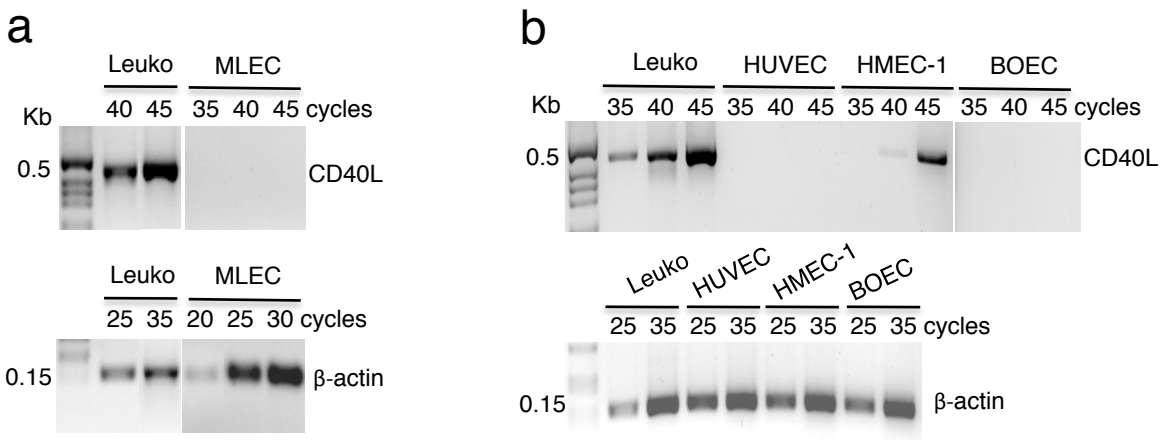
a
Leuko
MLEC
Kb
40 45 35 40 45 cycles
0.5
CD40L
Leuko
MLEC
25 35 20 25 30 cycles
0.15
β-actin
b
Leuko
HUVEC
HMEC-1
BOEC
Kb
35 40 45 35 40 45 35 40 45 35 40 45 cycles
0.5
CD40L
Leuko
HUVEC
HMEC-1
BOEC
25 35 25 35 25 35 25 35 cycles
0.15
β-actin

Fig. 6

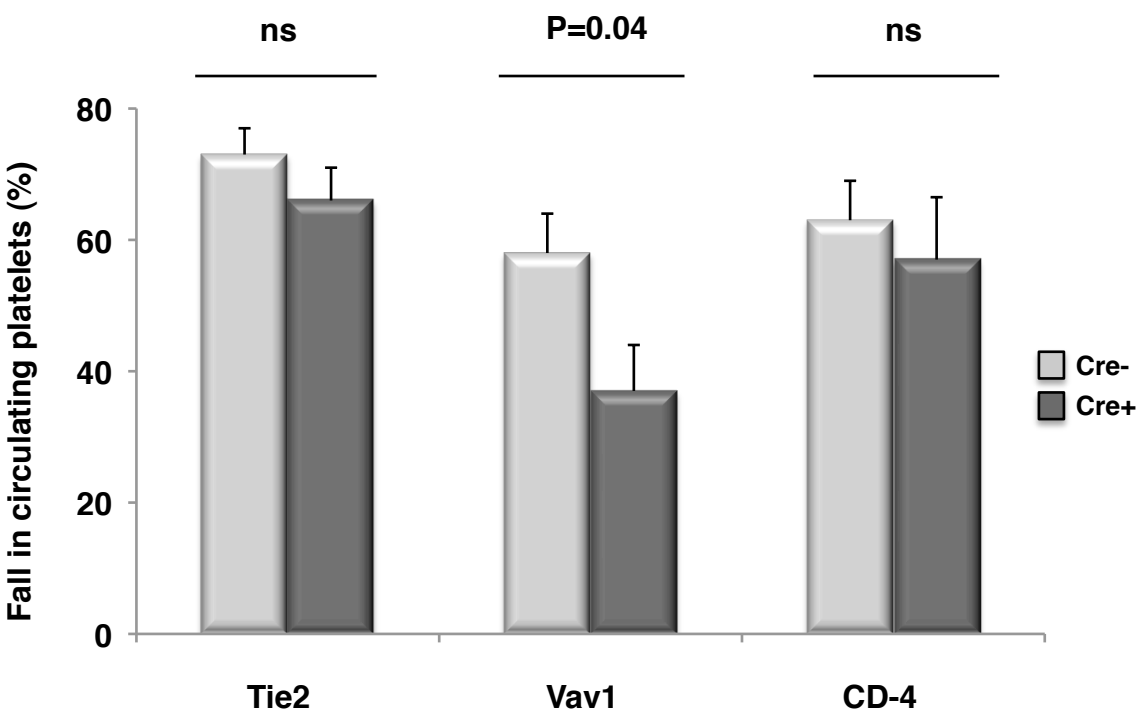
ns
P=0.04
ns
Fall in circulating platelets (%)
80
60
40
20
0
Tie2
Vav1
CD-4
Cre-
Cre+

Figure 7

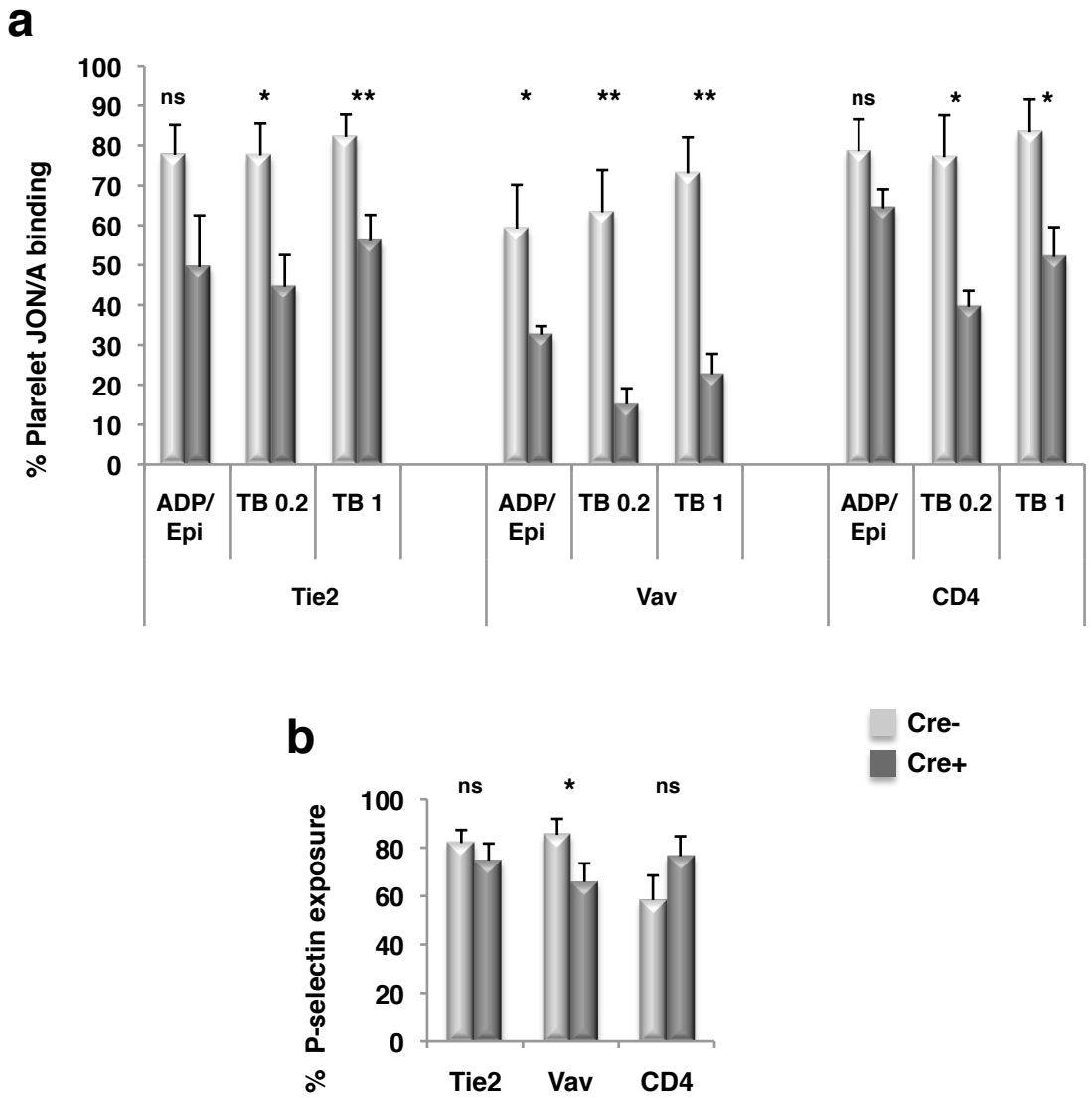
a
% Plarelet JON/A binding
100
90
80
70
60
50
40
30
20
10
0
ns
*
**
*
**
**
ns
*
*
ADP/ Epi
TB 0.2
TB 1
ADP/ Epi
TB 0.2
TB 1
ADP/ Epi
TB 0.2
TB 1
Tie2
Vav
CD4
b
Cre-
Cre+
% P-selectin exposure
100
80
60
40
20
0
ns
*
ns
Tie2
Vav
CD4

Figure 8

	Tie2-Cre		Vav-iCre		CD4-Cre	
	Cre- (n=14)	Cre+ (n=14)	Cre- (n=22)	Cre+ (n=19)	Cre- (n=12)	Cre+ (n=13)
RBC	7.3±0.3	7.6±0.2	6.9±0.2	7.1±0.3	7.2±0.4	7±0.4
HGB	10±0.5	11±0.3	9.6±0.4	10±0.5	10±0.5	9.5±0.5
HCT	31±1.6	32±0.9	29±0.1	30±1.1	29±1.5	28±1.7
MVC	42±0.4	43±0.3	42±0.3	42±0.4	41±0.3	41±0.3
RDWc	17±0.2	17±0.2	18±0.3	18±0.2	17±0.2	17±0.3
MCH	14±0.2	15±0.2	14±0.3	14±0.3	14±0.3	14±0.4
MCHC	33±0.5	34±0.6	33±0.7	33±0.7	34±0.7	34±0.8
PLT	290±20	251±22	340±20	339±25	287±16	269±26
WBC	4.3±0.4	5.1±0.5	4.3±0.4	3.2±0.3	4±0.5	4±0.3
LY	93±1.8	93±1.9	90±1.5	92±1	91±2.7	88±5
MI	4±1.1	2.4±0.4	3.4±0.6	3.7±0.7	2.4±0.6	2.7±0.4
GR	5±1.4	6±1.9	8.1±1.3	7.1±1.5	6.7±2.3	4.3±1.4

Table S1. Hemograms were determined in citrated blood samples obtained by cardiac puncture, using an automatic hemocytometer model Abacus Junior (Diatron, Diatron Messtechnik GmbH, Austria). Abbreviations (units): RBC, Red blood cells (M/nl); HGB, hemoglobin (g/dl); HCT, hematocrit (%); MVC, mean corpuscular value (fl); RDW, red cell distribution width (%); MCH, mean corpuscular hemoglobin (pg); MCHC, mean corpuscular hemoglobin concentration (%); PLT, platelets (k/ml); WBC, white blood cells (k/nl); LY, lymphocytes (%); MI, monocytes (%); GR, granulocytes (%). The values are mean ± standard error. There are no statistically significant differences as calculated by two tailed, unpaired t-test.

		Time (seconds) of	
		PT	aPTT
Tie2-Cre	Cre- (n)	18±1.6 (15)	32±5 (15)
	Cre+ (n)	17±0.9 (14)	46±10 (13)
	P	0.65	0.32
Vav-iCre	Cre- (n)	25±4.7 (11)	89±28 (9)
	Cre+ (n)	19.6±2.3 (11)	46.5±12 (11)
	P	0.31	0.15
CD4-Cre	Cre- (n)	25±4.2 (14)	27.6±4.3 (14)
	Cre+ (n)	21±4.2 (12)	33.4±6 (13)
	P	0.52	0.39

Table S2. Determination of prothrombin time (PT) and activated partial thromboplastin time (aPTT). PT and aPTT were measured in plasma samples using a coagulometrer model Start4 (Diagnostica Stago). Briefly, citrated-blood samples obtained through cardiac puncture were centrifuged at 2,500 g for 15 min and plasma was collected. PT time was determined after addition of 100 µl of Neoplastine CI Plus reagent (Diagnostica Stago) to a final volume of 50 µl of plasma. To measure aPTT time, 50 µl of plasma were mixed with the same volume of commercial aPTT Reagent (Diagnostica Stago) in the presence of $CaCl_2$ according to manufacture´s intructions.
The values are mean ± standard error, being n the number of observations. The value of P was calculated by two tailed, unpaired t-test.

		αIIbβ3	GPVI
Tie2-Cre	Cre-	113±13	5.4±0.4
	Cre+	96±3	5.2±0.2
Vav-iCre	Cre-	78±3	4.9±0.3
	Cre+	79±2.5	5.2±0.2
CD4-Cre	Cre-	83±2.3	4.3±0.03
	Cre+	80±4	4.6±0.2

Table S3. Platelet content of surface receptors. Washed platelets were incubated with FITC-labeled rat anti-mouse integrin αIIbβ3 and GPVI (Emfret Analytics, Eibelstadt, Germany) or control isotype-matched mouse IgGs for 30 minutes at room temperature. The samples were then washed and analyzed by flow cytometry. Values are mean channel fluorescence arbitrary units. The results are means ±SEM of 4 different observations in duplicate. Not significant differences were detected between control and CD40L-deficient platelets.